UDK 669.018.822:667.648.2:691.714.018.8
Original scientific article/Izvirni znanstveni članek

ISSN 1580-2949
MTAEC9, 52(4)383(2018)

CORROSION RESISTANCE OF SUPERHYDROPHILIC AND SUPERHYDROPHOBIC TiO_2/EPOXY COATINGS ON AISI 316L STAINLESS STEEL

KOROZIJSKA ODPORNOST SUPERHIDROFILNIH IN SUPERHIDROFOBNIH TiO_2/EPOKSI PREVLEK NA NERJAVNEM JEKLU AISI 316L

Aleksandra Kocijan, Marjetka Conradi, Črtomir Donik

Institute of Metals and Technology, Lepi pot 11, SI-1000 Ljubljana, Slovenia
aleksandra.kocijan@imt.si

Prejem rokopisa – received: 2017-11-15; sprejem za objavo – accepted for publication: 2018-01-09

doi:10.17222/mit.2017.191

Superhydrophilic and superhydrophobic TiO_2/epoxy coatings were prepared with as-received TiO_2 and fluoroalkylsilane (FAS) functionalised TiO_2 nanoparticles and successfully applied to the surface of AISI 316L stainless steel. The wetting properties of the coatings were confirmed with static contact-angle measurements. The corrosion performance of the investigated coatings was studied by electrochemical impedance spectroscopy (EIS). The open-circuit impedance spectra of the AISI 316L stainless steel, the epoxy-coated AISI 316L, the as-received TiO_2/epoxy coating on AISI 316L and the FAS-TiO_2/epoxy coating on AISI 316L were measured in simulated physiological Hank's solution. Bode plots and Nyquist diagrams were used to evaluate the corrosion properties of the investigated coatings. The results show the enhanced corrosion resistance of surface-modified stainless steel, especially in the case of the superhydrophobic FAS-TiO_2/epoxy coating.

Keywords: stainless steel, epoxy coating, TiO_2, electrochemistry

Superhidrofilne in superhidrofobne TiO_2/epoksi prevleke smo pripravili s TiO_2 in fluoroalkilsilan (FAS)-TiO_2 nanodelci in jih uspešno nanesli na površino nerjavnega jekla AISI 316L. Omočitvene lastnosti prevlek smo potrdili z meritvami kontaktnih kotov. Korozijske lastnosti pripravljenih prevlek smo raziskovali s pomočjo elektrokemijske impedančne spektroskopije (EIS). Impedančne spektre pri potencialu odprtega kroga smo merili na jeklu, epoksi prevleki ter superhidrofobni in superhidrofilni TiO_2/epoksi prevleki v simulirani fiziološki raztopini (Hankovi raztopini). Korozijske lastnosti omenjenih prevlek smo preučevali s pomočjo Bodejevih in Nyquistovih diagramov. Rezultati so pokazali izboljšano korozijsko odpornost površinsko obdelanega nerjavnega jekla, najbolj izrazito v primeru superhidrofobne FAS-TiO_2/epoksi prevleke.

Ključne besede: nerjavno jeklo, epoksi prevleka, TiO_2, elektrokemija

1 INTRODUCTION

Stainless steels, especially AISI 316L, are commonly used materials in biomedical applications because of their superior mechanical properties, high corrosion resistance and good biocompatibility.[1] However, an increasing number of clinical procedures are requiring the development of materials with superior performance and higher reliability.[2] Polymer coatings are known to improve the surface characteristics of the metallic substrate. Epoxy resins are used in various applications including the automotive, aircraft, maritime, flooring, food and medical industries because of their good chemical resistance, mechanical properties, strong adhesion with the substrate and corrosion protection by providing an effective physical barrier between the metal and the biological environment.[3,4] However, to avoid their susceptibility to abrasion[5] and poor resistance to crack propagation, due to a highly cross-linked structure,[6] the basic idea is to enhance the mechanical properties and to promote the surface compatibility of the coating by incorporating different nanofillers.[7–16] It is mainly the favourable effects of the particle size, the volume fraction and the size distribution on the mechanical properties of composite coatings that have been studied.[17–22] Z. Rubab et al. showed that sub-micron TiO_2 particles significantly enhance the glass-transition temperature, thermal oxidative stability, tensile strength and Young's modulus of epoxy polymers.[12] Hierarchical structures with a different nanoparticle size distribution influence the wetting properties of the surface.[13] Additionally, the incorporation of inorganic nanoparticles improves the barrier properties of the coatings by decreasing the porosity and increasing the path of aggressive ions and therefore enhancing the corrosion stability of the metallic substrate.[23]

In the present study we prepared superhydrophilic and superhydrophobic coatings with as-received and surface-modified TiO_2 nanoparticles, respectively. We focused on a comparison of the corrosion properties of epoxy coatings on AISI 316L stainless steel with an emphasis on tuning the wetting properties between the two limiting cases, superhydrophobic/superhydrophilic coatings. The corrosion properties were evaluated by

electrochemical impedance spectroscopy (EIS) and compared with the characteristics of bare and epoxy-coated AISI 316L stainless steel.

2 EXPERIMENTAL PART

Materials. • Austenitic stainless steel AISI 316L (17 % Cr, 10 % Ni, 2.1 % Mo, 1.4 % Mn, 0.38 % Si, 0.041 % P, 0.021 % C, < 0.005 % S in mass fraction) was used as a substrate. The steel sheet with a thickness of 1.5 mm was cut into discs of 25-mm diameter. The steel discs were grinded mechanically with SiC emery paper (up to 4000 grit), diamond polished (up to 1 μm), ultrasonically cleaned with ethanol and dried in warm air.

A two-component USP Class VI biocompatible epoxy EPO-TEK 302-3M (EPOXY TECHNOLOGY, Inc.) was mixed in the *w*/% ratio 100:45. TiO_2 nanoparticles with mean diameters of 30 nm were provided by Cinkarna Celje, whereas the 300-nm particles were supplied by US Research Nanomaterials, Inc. The TiO_2 particles were functionalized in 1 % of volume fraction of fluoroalkylsilane or FAS17 ($C_{16}H_{19}F_{17}O_3Si$) ethanol solution. The solution was shaken for a few minutes and left overnight prior to the use in the experiments. Prior to the TiO_2 nanoparticle adsorption, the diamond-polished AISI 316L substrate was spin-coated with an epoxy layer and then cured for 3 h at 65 °C. We decided on a base epoxy layer to improve the TiO_2 nanoparticle adhesion as the oxide layer growing on the surface of the clean AISI 316L substrate prevents adhesion and is very difficult to remove. The nanoparticles were further applied to the epoxy-coated AISI 316L surface by spin-coating 20 μL of 3 % of mass fractions of TiO_2 nanoparticle ethanol solution. We consecutively applied three deposits of dual-size, dual-layer coating consisting of 30-nm and 300-nm FAS-TiO_2 nanoparticles. The coating was then dried in an oven for approximately 30 min at 100 °C. The same procedure was repeated with the as-received, non-functionalized TiO_2 nanoparticles.

Contact-angle measurements. • The static contact-angle measurements of water (W) on a clean AISI 316L diamond-polished sample, on the epoxy-coated AISI 316L substrate, on the TiO_2/epoxy-coated AISI 316L substrate and on the FAS-TiO_2/epoxy-coated AISI 316L substrate were performed using a surface-energy evaluation system (Advex Instruments s.r.o.) at 20 °C and ambient humidity.

Electrochemical measurements. • Electrochemical measurements were performed on diamond-polished AISI 316L stainless steel, on the epoxy-coated AISI 316L substrate, on the TiO_2/epoxy-coated AISI 316L substrate and on the FAS-TiO_2/epoxy-coated AISI 316L substrate. The experiments were carried out in simulated physiological Hank's solution at pH = 7.8 and at room temperature (**Table 1**). All the chemicals were from Merck, Darmstadt, Germany. The measurements were performed using a three-electrode, flat BioLogic corrosion cell (volume 0.25 L). The test specimen was employed as the working electrode (WE), the exposed area of the sample was 1 cm^2. The reference electrode (RE) was a saturated calomel electrode (SCE, 0.242 V vs. SHE) and the counter electrode (CE) was a platinum net. Electrochemical measurements were recorded using a BioLogic Modular Research Grade Potentiostat/Galvanostat/FRA Model SP-300 with an EC-Lab Software. Long-term open-circuit *potentiostatic electrochemical impedance spectra* (EIS) were obtained for the investigated samples. The impedance was measured at the OCP, with a sinus amplitude of 5-mV peak-to-peak and a frequency range of 65 kHz to 1 mHz, directly after immersion for (1, 2, 3, 4, 16, 40, 64, 88, 112, 136 and 168) h. All the measurements were made at room temperature and were repeated at least three times. The data was collected and analysed by the EC-Lab V10.44 software from Bio-Logic Instruments. The impedance data are presented in terms of Bode and Nyquist plots. For the fitting process Zview v3.4d Scribner Associates software was used.

Table 1: Chemical composition of the simulated physiological Hank's solution

Reagent	*c* (g/L)
NaCl	8.0
KCl	0.40
$NaHCO_3$	0.35
$NaH_2PO_4 \cdot 2H_2O$	0.25
$Na_2HPO_4 \cdot 2H_2O$	0.06
$CaCl_2 \cdot 2H_2O$	0.19
$MgCl_2 \cdot 6H_2O$	0.41
$MgSO_4 \cdot 7H_2O$	0.06
glucose	1.0

3 RESULTS AND DISCUSSION

With the contact-angle measurements we confirmed the synthesis of the two limiting cases of coatings concerning their wetting characteristics. The FAS-TiO_2/epoxy coating was superhydrophobic with a contact angle above 150° and the as-received TiO_2/epoxy coating was superhydrophilic with a contact angle below 3°.

The corrosion performance of the investigated coatings was studied by EIS. The open-circuit impedance spectra of the AISI 316L stainless steel, the epoxy-coated AISI 316L, the as-received TiO_2/epoxy coating on AISI 316L and the FAS-TiO_2/epoxy coating on AISI 316L were measured over a 168 h immersion period in the simulated physiological Hank's solution.

Figures 1–3 show the EIS Bode plots and **Figures 4** to **6** the Nyquist diagrams for all the investigated coatings after 1 h, 1 d and 7 d of immersion in Hank's solution. The results for bare AISI 316L stainless steel after 1 h, 1 d and 7 d of immersion in Hank's solution were used for comparison. In the case of the investigated

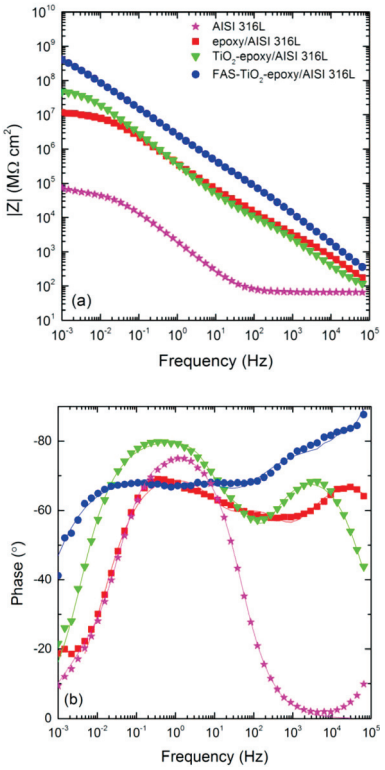

Figure 1: EIS Bode plot of AISI 316L stainless steel, the epoxy coating, as-received TiO_2/epoxy coating and the FAS-TiO_2/epoxy coating on the surface of AISI 316L stainless steel in Hank's solution after 1 h of immersion

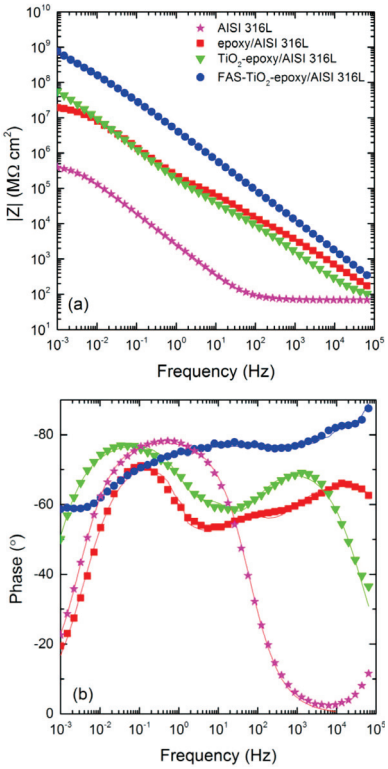

Figure 2: EIS Bode plot of AISI 316L stainless steel, the epoxy coating, as-received TiO_2/epoxy coating and the FAS-TiO_2/epoxy coating on the surface of AISI 316L stainless steel in Hank's solution after 1 d of immersion

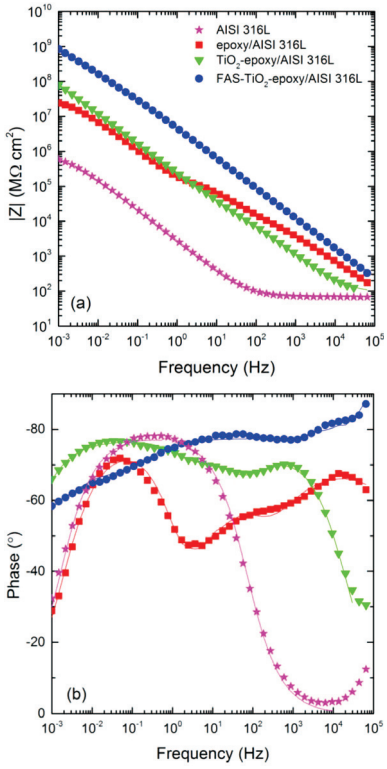

Figure 3: EIS Bode plot of AISI 316L stainless steel, the epoxy coating, as-received TiO_2/epoxy coating and the FAS-TiO_2/epoxy coating on the surface of AISI 316L stainless steel in Hank's solution after 7 d of immersion

coatings on AISI 316L stainless steel, the first time constant in the high-frequency range was associated with the barrier properties of the coatings, the second time constant in the medium frequency range with the formation of an oxide layer at the coating/ substrate interface and the third time constant in the low-frequency

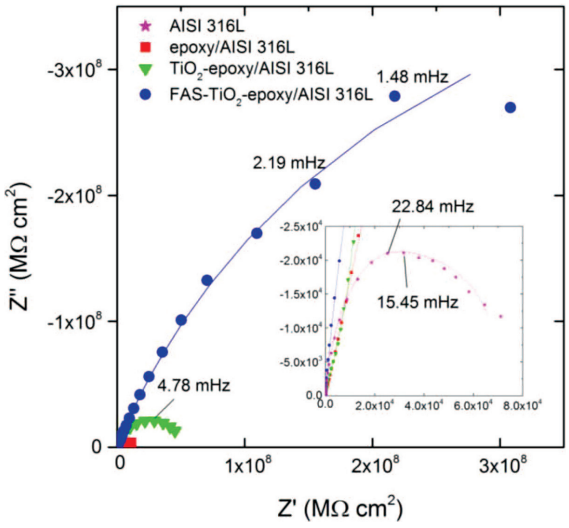

Figure 4: Nyquist diagram of AISI 316L stainless steel, the epoxy coating, as-received TiO_2/epoxy coating and the FAS-TiO_2/epoxy coating on the surface of AISI 316L stainless steel in Hank's solution after 1 h of immersion. The inset diagrams represent the high-frequency range of the impedance responses

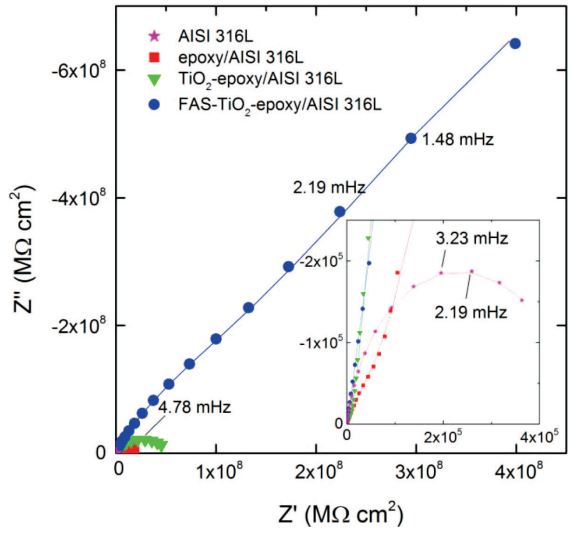

Figure 5: Nyquist diagram of AISI 316L stainless steel, the epoxy coating, as-received TiO_2/epoxy coating and the FAS-TiO_2/epoxy coating on the surface of AISI 316L stainless steel in Hank's solution after 1 d of immersion; the inset diagrams represent the high-frequency range of impedance responses

range with the corrosion of the substrate.[24] In the case of AISI 316L stainless steel, the spectra were characterised by two time constants. The first time constant in the high-medium frequency range was assigned to the resistance due to the ionic paths through the oxide film and the low-medium-frequency time constant was correlated with the charge-transfer process.[8,25,26] Magnitude plots revealed that the total impedance for all three investigated coatings increased compared to the bare alloy, the values increased from 10^6 Ω cm^2 for AISI 316L to 10^7 Ω cm^2 for the epoxy-coated AISI 316L, 10^8 Ω cm^2 for the as-received TiO_2/epoxy-coated AISI 316L and 10^9 Ω cm^2 for the FAS-TiO_2/ epoxy-coated AISI 316L. This indicated the higher corrosion stability of the coated samples, especially with the addition of TiO_2 nanoparticles. Furthermore, a high-frequency time constant was clearly observed for all the investigated coatings compared to the bare AISI 316L, thus indicating the barrier ability of the coatings. This effect was more pronounced for the FAS-TiO_2/epoxy coating with the phase angle approaching –90°, which is typical of the capacitor and is ascribed to the capacitive behaviour of the coating.

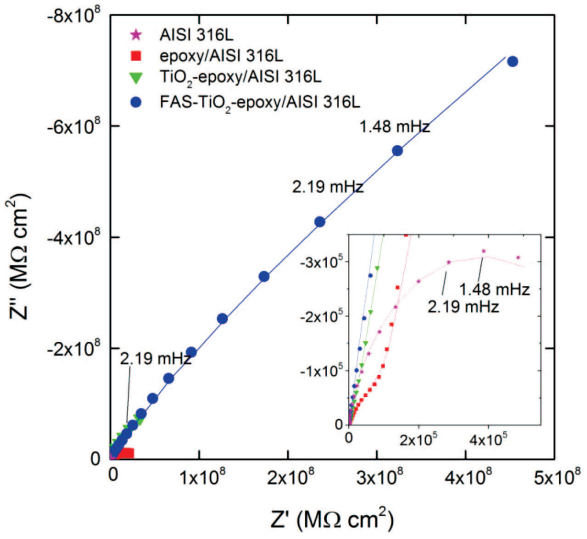

Figure 6: Nyquist diagram of AISI 316L stainless steel, the epoxy coating, as-received TiO_2/epoxy coating and the FAS-TiO_2/epoxy coating on the surface of AISI 316L stainless steel in Hank's solution after 7 d of immersion; the inset diagrams represent the high-frequency range of impedance responses

Figure 7 presents the equivalent circuits that were used to fit the experimental data to the theoretical impedance data. The EIS technique enables us to match the electrochemical behaviour of the investigated system with model circuits consisting of specific components equivalent to the parameters of the electrochemical system.[27] We selected a model that provided the results with the smallest errors of fit. In the equivalent circuit applied for the evaluation of the investigated coatings R_s refers to the solution resistance. High-frequency resistance (R_{pore}) was associated with the electrolyte in the pores of the coating, medium-frequency resistance (R_{ox}) was related to the interfacial oxide and low-frequency resistance (R_{sub}) reflected the corrosion process (**Figure 7a**). Each resistance was coupled with the CPE element, expressing the coating capacitance (CPE_{pore}), capacitance of the oxide layer (CPE_{ox}) and capacitance of the double layer (CPE_{sub}). The circuit was simplified to the one with two time constants up to 24 h of immersion due to the lower fitting errors (**Figure 7b**). In the case of AISI 316L stainless steel (**Figure 7c**), the spectra were characterised by two time constants, the first time constant in high-medium frequency range was simulated by the resistance due to the ionic paths through the oxide film (R_{ox}) and was coupled with a capacitive behaviour of the oxide film (CPE_{ox}). The low-medium-frequency time constant was correlated with the charge-transfer process, which was composed of charge-transfer resistance (R_{sub}) in parallel with the double-layer capacitance (CPE_{sub}).[8,24,26]

The evolution of the pore resistance (R_{pore}) revealed the barrier properties of the coatings (**Figure 8a**). We

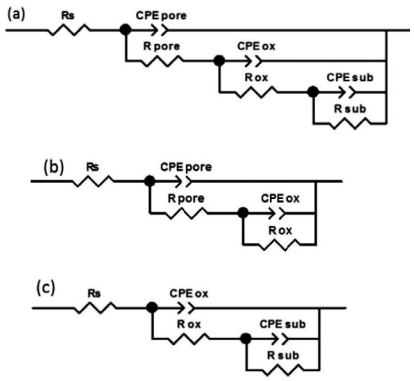

Figure 7: Equivalent electrical circuits for modelling the EIS data

observed that the R_{pore} values were the highest for the FAS-TiO_2/epoxy coating and the TiO_2/epoxy coating compared to the pure epoxy coating, indicating a better corrosion performance. Additionally, the R_{pore} of epoxy coating slightly decreased with the immersion time, probably due to the easier penetration of the electrolyte. The addition of TiO_2 nanoparticles to the epoxy coating prolongs the diffusion path of the ionic species through the coating.[8] The admittance of the CPE (**Table 2**) was in the range of 10^{-7} Ω^{-1} cm^{-2} s^n for the epoxy coating and the TiO_2/epoxy coating, and in the range of 10^{-8} Ω^{-1} cm^{-2} s^n for the FAS-TiO_2/epoxy coating. The values for all three coatings remained almost constant at different immersion times. The CPE exponent was above 0.88 for the FAS-TiO_2/epoxy coating, 0.84 for the TiO_2/epoxy coating, and 0.75 for the epoxy coating.

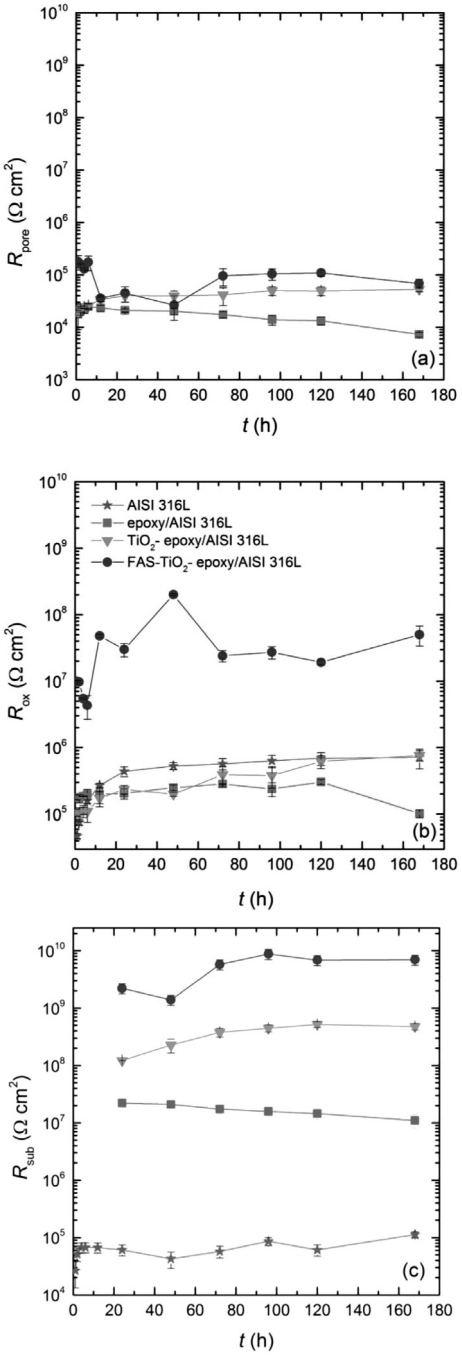

Figure 8: Evolution of resistance for bare AISI 316L stainless steel, the epoxy coating, as-received TiO_2/epoxy coating and the FAS-TiO_2/epoxy coating on AISI 316L stainless steel during immersion in Hank's solution

Table 2: Fitting parameters (admittances) for the epoxy coating, as-received TiO_2/epoxy coating and the FAS-TiO_2/epoxy coating on the surface of AISI 316L stainless steel after 24 h and 168 h of immersion in Hank's solution

t (h)	CPE_{pore} (Ω^{-1} cm^{-2} s^n)	CPE_{ox} (Ω^{-1} cm^{-2} s^n)	CPE_{sub} (Ω^{-1} cm^{-2} s^n)
Epoxy coated AISI 316L			
24	$5{,}1 \times 10^{-7}$	$2{,}1 \times 10^{-7}$	$6{,}5 \times 10^{-7}$
168	$5{,}6 \times 10^{-7}$	$2{,}0 \times 10^{-7}$	$1{,}9 \times 10^{-7}$
TiO_2/epoxy coated AISI 316L			
24	$2{,}6 \times 10^{-7}$	$2{,}9 \times 10^{-7}$	$2{,}4 \times 10^{-7}$
168	$2{,}1 \times 10^{-7}$	$1{,}1 \times 10^{-7}$	$1{,}0 \times 10^{-7}$
FAS-TiO_2/epoxy coated AISI 316L			
24	$2{,}9 \times 10^{-8}$	$5{,}0 \times 10^{-8}$	$1{,}4 \times 10^{-8}$
168	$2{,}3 \times 10^{-8}$	$9{,}4 \times 10^{-9}$	$1{,}3 \times 10^{-8}$

The resistance associated with the medium-frequency time constant (R_{ox}) (**Figure 8b**) had higher values, especially for the FAS-TiO_2/epoxy coating. The values for the TiO_2/epoxy coating were comparable to the pure epoxy coating. However, a slight increase for the TiO_2/epoxy coating compared to a slight decrease for pure epoxy coating was recorded, demonstrating improved protective interfacial properties by the addition of TiO_2 nanoparticles. The admittance of the CPE for the epoxy coating was approximately 10^{-7} Ω^{-1} cm^{-2} s^n and remained constant for different immersion times. The admittance of the CPE (**Table 2**) for the as-received TiO_2/epoxy coating was similar as for the epoxy coating, but slightly decreased with the immersion time. In the case of the FAS-TiO_2/epoxy coating, the admittance of the CPE decreased from 5×10^{-8} Ω^{-1} cm^{-2} s^n to 9×10^{-9} Ω^{-1} cm^{-2} s^n with the immersion time. The CPE exponent was in the range 0.75–0.80 for the FAS-TiO_2/epoxy coating, above 0.83 for the TiO_2/epoxy coating, and 0.80 for the epoxy coating.

The evolution of the low-frequency resistance (R_{sub}) is shown in **Figure 8c**. The low-frequency resistance was the highest for the FAS-TiO_2/epoxy and the TiO_2/epoxy coatings, indicating that the addition of nanoparticles, especially hydrophobic ones, increased the corrosion stability of the substrate. The values of R_{sub} slightly increased with the immersion time for the FAS-TiO_2/epoxy and the TiO_2/epoxy-coated samples compared to the pure epoxy coating. The admittance of the CPE (Table 2) for the epoxy coating was in the range of 6×10^{-7} Ω^{-1} cm^{-2} s^n and for the TiO_2/epoxy coating in the range of 2×10^{-7} Ω^{-1} cm^{-2} s^n. The admittance of the CPE for the FAS-TiO_2/epoxy coating was approximately 10^{-8} Ω^{-1} cm^{-2} s^n. All the values slightly decreased with the immersion

time. The CPE exponent was approximately 0.59 for the FAS-TiO_2/epoxy coating, 0.68 for the TiO_2/epoxy coating, and approximately 0.58 for the epoxy coating.

4 CONCLUSIONS

In this paper we presented the preparation of superhydrophobic FAS-TiO_2/epoxy and superhydrophilic as-received TiO_2/epoxy coatings on the surface of AISI 316L stainless steel. The electrochemical study was applied to study the barrier coatings of the prepared coatings in a simulated physiological solution. The obtained results show a significant improvement in terms of the corrosion stability of the epoxy coatings with the addition of TiO_2 nanoparticles compared to the pure epoxy coating, especially in the case of the surface-modified superhydrophobic TiO_2, manifesting in higher R values and lower CPE values. The addition of nanoparticles provides better barrier properties due to the prolonged penetration of the electrolyte through the coating.

Acknowledgments

The authors acknowledge the project (Antibacterial Nanostructured Surfaces for Biological Applications, ID J2-7196) was financially supported by the Slovenian Research Agency.

5 REFERENCES

[1] J. C. Yu, W. K. Ho, J. Lin, K. Y. Yip, P. K. Wong, Photocatalytic activity, antibacterial effect, and photoinduced hydrophilicity of TiO_2 films coated on a stainless steel substrate, Environmental Science & Technology, 37 (**2003**) 10, 2296–2301

[2] L. Visai, L. De Nardo, C. Punta, L. Melone, A. Cigada, M. Imbriani, C.R. Arciola, Titanium oxide antibacterial surfaces in biomedical devices, International Journal of Artificial Organs, 34 (**2011**) 9, 929–946

[3] F. Galliano, D. Landolt, Evaluation of corrosion protection properties of additives for waterborne epoxy coatings on steel, Progress in Organic Coatings, 44 (**2002**) 3, 217–225

[4] F. W. Liu, M. X. Yin, B. Y. Xiong, F. Zheng, W. F. Mao, Z. Chen, C. Q. He, X. P. Zhao, P. F. Fang, Evolution of microstructure of epoxy coating during UV degradation progress studied by slow positron annihilation spectroscopy and electrochemical impedance spectroscopy, Electrochimica Acta, 133 (**2014**), 283–293

[5] B. Wetzel, F. Haupert, M. Q. Zhang, Epoxy nanocomposites with high mechanical and tribological performance, Composites Science and Technology, 63 (**2003**) 14, 2055–2067

[6] S. Yamini, R. J. Young, Stability of crack-propagation in epoxy-resins, Polymer, 18 (**1977**) 10, 1075–1080

[7] M. Conradi, M. Zorko, A. Kocijan, I. Verpoest, Mechanical properties of epoxy composites reinforced with a low volume fraction of nanosilica fillers, Materials Chemistry and Physics, 137 (**2013**) 3, 910–915

[8] M. Conradi, A. Kocijan, D. Kek-Merl, M. Zorko, I. Verpoest, Mechanical and anticorrosion properties of nanosilica-filled epoxy-resin composite coatings, Applied Surface Science, 292 (**2014**), 432–437

[9] M. Conradi, A. Kocijan, M. Zorko, I. Verpoest, Damage resistance and anticorrosion properties of nanosilica-filled epoxy-resin composite coatings, Progress in Organic Coatings, 80 (**2015**), 20–26

[10] A. Afzal, H. M. Siddiqi, S. Saeed, Z. Ahmad, The Influence of Epoxy Functionalized Silica Nanoparticles on Stress Dispersion and Crack Resistance in Epoxy-Based Hybrids, Materials Express, 1 (**2011**) 4, 299–306

[11] S. S. Peng, W. J. Zhao, H. Li, Z. X. Zeng, Q. J. Xue, X. D. Wu, The enhancement of benzotriazole on epoxy functionalized silica sol-gel coating for copper protection, Applied Surface Science, 276 (**2013**), 284–290

[12] Z. Rubab, A. Afzal, H. M. Siddiqi, S. Saeed, Preparation, Characterization, and Enhanced Thermal and Mechanical Properties of Epoxy-Titania Composites, Scientific World Journal (**2014**)

[13] H. A. Al-Turaif, Effect of nano TiO2 particle size on mechanical properties of cured epoxy resin, Progress in Organic Coatings, 69 (**2010**) 3, 241–246

[14] A. Kubacka, M. S. Diez, D. Rojo, R. Bargiela, S. Ciordia, I. Zapico, J. P. Albar, C. Barbas, V. A. P. M. dos Santos, M. Fernandez-Garcia, M. Ferrer, Understanding the antimicrobial mechanism of TiO_2-based nanocomposite films in a pathogenic bacterium, Scientific Reports, 4 (**2014**)

[15] X. Wei, Z. Yang, S. L. Tay, W. Gao, Photocatalytic TiO_2 nanoparticles enhanced polymer antimicrobial coating, Applied Surface Science, 290 (**2014**), 274–279

[16] M.-Y. Lan, C.-P. Liu, H.-H. Huang, S.-W. Lee, Both Enhanced Biocompatibility and Antibacterial Activity in Ag-Decorated TiO_2 Nanotubes, Plos One, 8 (**2013**) 10

[17] A. C. Moloney, H. H. Kausch, T. Kaiser, H. R. Beer, Parameters determining the strength and toughness of particulate filled epoxide-resins, Journal of Materials Science, 22 (**1987**) 2, 381–393

[18] M. Frounchi, T. A. Westgate, R. P. Chaplin, R. P. Burford, Fracture of polymer networks based on diethylene glycol bis(allyl carbonate), Polymer, 35 (**1994**) 23, 5041–5045

[19] F. Stricker, Y. Thomann, R. Mulhaupt, Influence of rubber particle size on mechanical properties of polypropylene-SEBS blends, Journal of Applied Polymer Science, 68 (**1998**) 12, 1891–1901

[20] R. T. Quazi, S. N. Bhattacharya, E. Kosior, The effect of dispersed paint particles on the mechanical properties of rubber toughened polypropylene composites, Journal of Materials Science, 34 (**1999**) 3, 607–614

[21] T. Adachi, W. Araki, T. Nakahara, A. Yamaji, M. Gamou, Fracture toughness of silica particulate-filled epoxy composite, Journal of Applied Polymer Science, 86 (**2002**) 9, 2261–2265

[22] G. Zhang, R. Sebastian, T. Burkhart, K. Friedrich, Role of monodispersed nanoparticles on the tribological behavior of conventional epoxy composites filled with carbon fibers and graphite lubricants, Wear, 292 (**2012**), 176–187

[23] B. Ramezanzadeh, S. Niroumandrad, A. Ahmadi, M. Mahdavian, M. H. Mohamadzadeh Moghadam, Enhancement of barrier and corrosion protection performance of an epoxy coating through wet transfer of amino functionalized graphene oxide, Corrosion Science, 103 (**2016**), 283–304, doi:10.1016/j.corsci.2015.11.033

[24] A. C. Balaskas, I. A. Kartsonakis, D. Snihirova, M. F. Montemor, G. Kordas, Improving the corrosion protection properties of organically modified silicate-epoxy coatings by incorporation of organic and inorganic inhibitors, Progress in Organic Coatings, 72 (**2011**) 4, 653–662

[25] A. Kocijan, D. K. Merl, M. Jenko, The corrosion behaviour of austenitic and duplex stainless steels in artificial saliva with the addition of fluoride, Corrosion Science, 53 (**2011**) 2, 776–783

[26] D. D. Macdonald, The point-defect model for the passive state, Journal of the Electrochemical Society, 139 (**1992**) 12, 3434–3449

[27] J. R. M. E. Barsoukov (Ed.), Impedance Spectroscopy: Theory, Experiment, and Applications, John Wiley & Sons Inc., Hoboken, NJ, 2005